DOI: 10.1002/asia.200700180

Spectrum–Structure Relationship in Carbohydrate Vibrational Circular Dichroism and Its Application to Glycoconjugates

Tohru Taniguchi and Kenji Monde*[a]

Abstract: Preliminary reports of the nature of the vibrational circular dichroism (VCD) peak at around 1145 cm^{-1}, which is characteristic of axial glycosidic sugars and is called the glycoside band (*J. Am. Chem. Soc.* **2004**, *126*, 9496), have been throughly examined. Through systematic carbohydrate measurements, it was found that the sign of the glycoside band reflects not only the anomeric configuration but also the pyranose conformation. Isotope and theoretical studies characterized its vibrational mode as C1–H1 deformation coupled with C1–O1 stretching, which indicates its applicability to more-complicated glycoconjugates. In this study, for the first time, carbohydrate VCD spectra were reliably predicted by means of density functional theory (DFT) calculations. The VCD technique was applied to glycopeptides, and simultaneous analysis of both the carbohydrate and aglycan parts was carried out.

Keywords: ab initio calculations · carbohydrates · glycoconjugates · structure elucidation · vibrational circular dichroism

Introduction

Carbohydrates are extremely diverse molecules that include polysaccharides, nucleotides, glycoproteins, glycolipids, and glycosylated natural products. Their structural complexity is closely related to their multiple biological functions such as immune defense, viral infection, cell adhesion, protein regulation, and fertilization.[1] Carbohydrates are made up of monosaccharide residues connected through glycosidic linkages. Much synthetic effort has been made in the stereoselective construction of glycoside bonds, that is, α or β configuration.[2] The anomeric configuration regulates recognition, stability, and secondary structure, as is widely investigated in various fields from drug development to food digestion.[2a,3] For these reasons, the determination of anomeric stereochemistry is a key step in the structural analysis of natural as well as synthetic carbohydrates.

Due to the diversity of carbohydrates, structural studies of these compounds are not as straightforward as those of proteins and DNA and require several complementary methods such as NMR spectroscopy and MS instead of just automatic analysis. Although NMR spectroscopy has been widely used,[4] it is limited to small molecules such as oligosaccharides, and the acquisition and interpretation of NMR spectra is time-consuming. On the other hand, MS methods have become quite advanced in recent decades,[5] and glycan structures have been successfully characterized by using the tandem-MS technique (MS^n). However, because carbohydrate MS analysis observes fragmentation at the glycosidic linkage, information about the anomeric configuration is ambiguous. This is also the case in analysis by conventional permethylation,[6,7] in which the glycoside bonds are cleaved and, therefore, the anomeric configurations of the original compounds are impossible to assign. The development of further techniques is imperative in this rapidly progressing glycoscience field.

A carbohydrate molecule is an assembly of chiral carbon atoms, but the aforementioned methods are based on achiral theory, which does not extract chiral structural information. Optical rotation, a chiroptical technique with the longest history, was used for an anomeric configuration study of mainly monosaccharides.[8] Recently, vibrational circular dichroism (VCD) spectroscopy has seen significant instrumental and theoretical advances that allow the routine investigation of carbohydrates. VCD spectroscopy measures the dif-

[a] Dr. T. Taniguchi, Prof. K. Monde
Laboratory of Advanced Chemical Biology
Graduate School of Advanced Life Science
Frontier Research Center for Post-Genome Science and Technology
Hokkaido University, Kita-ku, Sapporo 001-0021 (Japan)
Fax: (+81) 11-706-9042
E-mail: kmonde@glyco.sci.hokudai.ac.jp

Supporting information for this article is available on the WWW under http://www.chemasianj.org or from the author.

 © 2007 Wiley-VCH Verlag GmbH & Co. KGaA, Weinheim

ferential absorption of a chiral sample for left versus right circularly polarized infrared light associated with vibrational transitions.[9,10] As all carbohydrates show IR absorption, VCD spectroscopy as well as Raman optical activity (ROA),[11] the Raman counterpart of the former, are promising chiroptical analysis tools that can extract carbohydrate stereochemical information without derivatization. In contrast to the widely studied proteins and nucleic acids, however, only a limited number of VCD applications to carbohydrates have been reported, partly due to a scarcity of appropriate samples. Furthermore, simple monosaccharides are devoid of a carbonyl moiety; thus, the accessible mid-IR region is confined to a frequency of less than 1500 cm^{-1},[12] where broad and relatively weak VCD features have been observed, thus hampering the establishment of an unambiguous structure–spectrum relationship. This situation may be compared to polypeptides and nucleic acids, which exhibit characteristic amide VCD signals indicative of their structures.[13] Interpretation of VCD spectra of proteins and nucleic acids has been aided by theoretical calculation,[14] but, in the case of carbohydrates, the theoretical approach faces difficulties in managing their flexibility and solvent effects.

However, the high sensitivity of VCD spectroscopy to even subtle structural changes recognized in the previous sugar VCD reports[12] stimulated us to conduct an extensive VCD study on carbohydrates. In the course of the construction of a comprehensive carbohydrate VCD database, we recently discovered the first carbohydrate structure–VCD-spectrum relationship; we characterized the anomeric configuration and named its signal the "glycoside band". This band was preliminarily defined as a negative, sharp, and intense VCD band at around 1145 cm^{-1}, exhibited by D-sugars with an axial α-glycosidic linkage (Figure 1).[15] The band was observed for methyl α-glycosides (R_1 = OMe and R_2 = H; Figure 1) of D-glucose (**2a**), D-galactose (**3a**), D-xylose (**4a**), D-mannose (**6a**), and 2-acetamide-2-deoxy-D-glucose (**7a**), which suggests that this band may be observable in other sugar species. Furthermore, the VCD spectra of a set of D-glucobioses, α-D-glucose (**2c**) and β-D-glucose (**2d**), imply the generality of the glycoside band for the various types of carbon atoms involved in the glycosidic linkages, that is, methyl (**2a–10a** in Figure 1), methylene (the α-1,6-linked glucobiose), methine (the other α-linked glucobioses), or even just a proton (**2c**). Taking advantage of the high signal intensity of this band, we further demonstrated

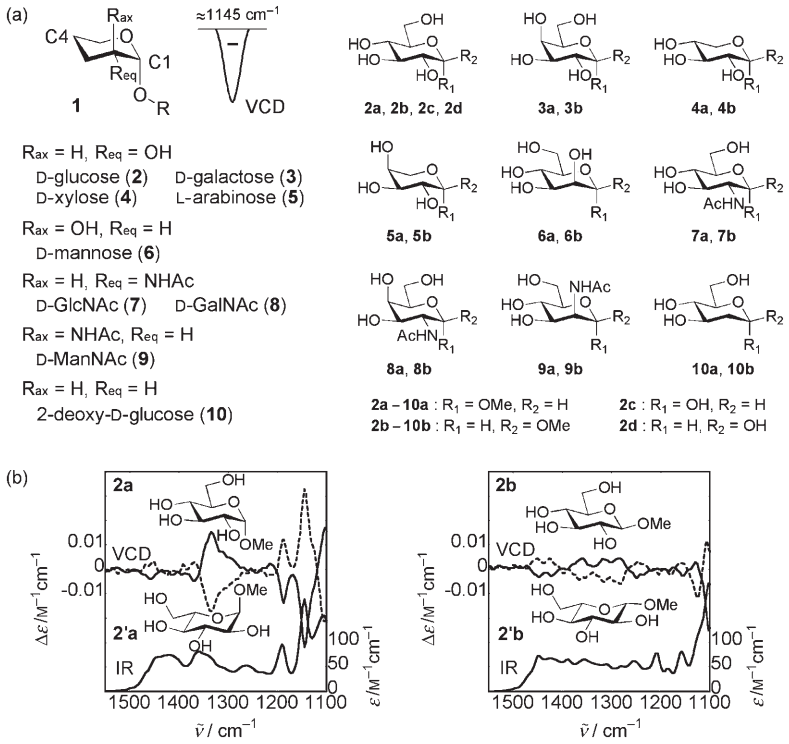

Figure 1. a) Preliminarily proposed structural motif exhibiting a negative sharp band at around 1145 cm^{-1} (the negative glycoside band). R represents the glycosyl acceptor, but it can be just a proton (R = H) or a methyl group (R = Me). Each monosaccharide structure is shown on the right, in which **2a–10a** and **2c** are α-D-sugars and **2b–10b** and **2d** are β-D-sugars except for **5a** (methyl β-L-arabinopyranoside) and **5b** (methyl α-L-arabinopyranoside). In the first part of this paper, it was found that the glycoside band was observable irrespective of the substituents at C2 (R_{ax} and R_{eq}). In the last part, R was substituted for an ordered peptide. b) Representative VCD (top) and IR spectra (bottom) of axial and equatorial glycosides (solid line = **2a** and **2b**, dashed line = **2'a** and **2'b**). At 1146 cm^{-1}, only **2a** (axial glycoside with the $^4C_1$ conformation) exhibited a negative, sharp, intense VCD peak, that is, the glycoside band. These spectra were obtained in [D_6]DMSO (c = 0.16 M, l = 72 μm; DMSO = dimethyl sulfoxide) for 3 h. For the spectra of the other sugars, see the Supporting Information.

Abstract in Japanese:

以前報告した 1145 cm^{-1} 付近に観測されるアキシアルグリコシド特異的な VCD ピーク、すなわち glycoside band（*J. Am. Chem. Soc.* **2004**, *126*, 9496）について詳細に検討したので報告する。各種糖の VCD スペクトルを系統的に測定し、glycoside band の符号がアノマー立体化学のみならずピラノース六員環のコンフォメーションを反映することを見出した。同位体置換実験と理論計算により、本バンドの振動モードは C1–H1 変角振動と C1–O1 伸縮振動の結合型であると帰属され、さらに複雑な複合糖質への応用性が示された。なお、本研究は DFT 計算により糖 VCD 予測を信頼性高く行った最初の報告例である。最後に、糖ペプチドへと VCD を応用し、糖部分とペプチド部分の両方が同時に解析可能であることを示した。

 © 2007 Wiley-VCH Verlag GmbH & Co. KGaA, Weinheim

the first monitoring of an enzymatic reaction with VCD spectroscopy. However, there has been no insight into the vibrational mode of the glycoside band. Because this characteristic feature can potentially advance the use of VCD spectroscopy in this field, and because the effectiveness of vibrational optical activity techniques in the study of glycoproteins was recently indicated by means of ROA,[11a] a detailed understanding of this band is essential for further VCD application to carbohydrate structural analysis. Herein, we describe the nature of the glycoside band, including its vibrational mode and ability to characterize conformation, through systematic carbohydrate VCD measurements, isotope experiments, and theoretical calculations on model compounds. In this study, for the first time, carbohydrate VCD spectra were reliably interpreted by density functional theory (DFT) calculations.[16] Finally, VCD spectroscopy was applied to glycopeptides, thus demonstrating the broad applicability of this band to glycoconjugates and allowing the simultaneous structural analysis of carbohydrate and aglycan parts.

Results and Discussion

Differences in the Glycoside Bands of $^4C_1$ and $^1C_4$ Sugars

The VCD spectra of the axial methyl glycosides **2a**–**5a** and the equatorial counterparts **2b**–**5b** were obtained in the mid-IR region.[30] The glycoside band was commonly observed for the axial glycosidic species but not for the equatorial. Comparison of **2a** with **3a** and **4a** suggests that this band is independent of the C4 and C6 substituents. This is also the case with **5a**, which is designated a β-L-sugar.

Several other L-sugars with axial glycosidic linkage, such as methyl α-L-glucopyranoside (**2′a**; Figure 1), L-galactose (**3′**), L-fucose (**11**), and methyl α-L-fucopyranoside (**11a**)

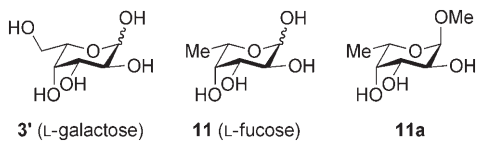

Scheme 1. Structures of the $^1C_4$ sugars that exhibited the positive glycoside band. For the spectra of these sugars, see the Supporting Information.

(Scheme 1), exhibited positive glycoside bands.[30] From these data, the type of pyranose-ring conformation ($^4C_1$ or $^1C_4$) and the direction of the glycoside (axial or equatorial), rather than the D/L and α/β designations, should be included in the definition of the glycoside band.[17] Thus, a negative glycoside band was observed for an axial glycosidic sugar in the $^4C_1$ conformation, whereas a positive band was seen for that in the $^1C_4$ form. Consequently, it is suggested that not only the anomeric configuration but also the pyranose-ring conformation can be distinguished by using the glycoside band.

Independence of the Glycoside Band from C2 Substituents

To utilize the glycoside band optimally for carbohydrate structural analysis, it is crucial to gain sufficient insight into its vibrational mode as well as its scope and limitations. We next examined the influence of the C2 substituents (R_{ax} and R_{eq}) as this band was assumed to relate to the anomeric center (C1); at this point, the closest carbon atom, C2, can perturb this band. Moreover, R_{ax} and R_{eq} in biological carbohydrates are more variable than the other carbon atoms (Figure 1), so the applicability of the technique in such systems should be investigated.

VCD spectra of methyl α-glycosides **6a**–**10a** (**6**: R_{ax} = OH, R_{eq} = H; **7** and **8**: R_{ax} = H, R_{eq} = NHAc; **9**: R_{ax} = NHAc, R_{eq} = H; **10**: R_{ax} = H, R_{eq} = H) were obtained, and all of them showed the negative glycoside band.[30] These results demonstrate the generality of this band for various patterns of R_{ax} and R_{eq}.

Isotope Experiment

The independence of the glycoside band from the substituents on C2–C6 indicates that it stems mainly from vibrational motions that involve the anomeric carbon atoms and atoms in its close vicinity. To identify the vibrational mode in more detail, we considered two approaches. The first was isotope labeling, which was used to interpret the VCD spectra of biomolecules.[14b,18] If the absorption of interest originates primarily from a diatomic stretching movement, the approximate frequency shift can be predicted by the Hooke law.[19] However, isotopic assignment often becomes inefficient or ambiguous in cases in which more than two atoms contribute significantly to the vibrational transition. The second approach used was the recently developed DFT calculations,[16] which gives the vibrational modes that correspond to each absorption. The latter approach was limited to relatively simple molecules or model compounds of the complicated targets.

Our primary attempt was the isotopic substitution of the anomeric oxygen atom (O1) of methyl α-D-glucopyranoside (Figure 2a). The ^{18}O-labeled **12** exhibited the glycoside band at a frequency 5 cm^{-1} lower than the unlabeled **2a**, thus implying the involvement of O1 in this vibrational transition. This vibration would not be a simple diatomic C–O stretching movement as the shift is too small compared to that of about 30 cm^{-1} predicted by the Hooke law. We next prepared 1-deuterated methyl α-D-glucopyranoside (**13**) starting from 1-[D]glucose and methanol. Unexpectedly, **13** exhibited dramatically different spectral patterns from those of **2a** in the glycoside-band region (Figure 2b). The glycoside band shifted to 1136 cm^{-1} with decreased intensity or to below 1100 cm^{-1}, or disappeared due to complete change of the vibrational mode. In any case, the result strongly indicated significant participation of H1 in the glycoside-band absorption. This absorption cannot be assigned as a diatomic C1–H1 stretch because C–H stretches are observed at around 3000 cm^{-1}, and we recently assigned the C1–H1

 © 2007 Wiley-VCH Verlag GmbH & Co. KGaA, Weinheim

CHEMISTRY
AN ASIAN JOURNAL

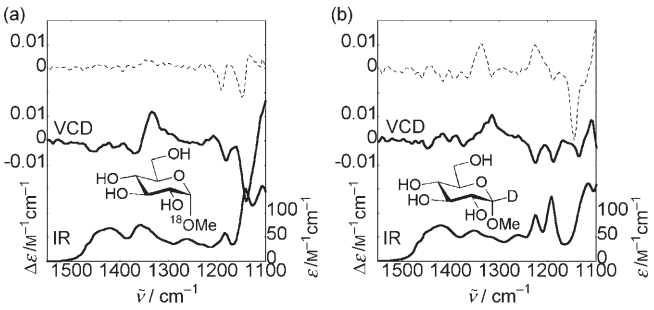

Figure 2. VCD (middle) and IR spectra (bottom) of isotopomers in [D$_6$]DMSO (c = 0.16 M, l = 72 μm, BaF$_2$ cell) and difference VCD spectra (dashed line) between unlabeled methyl α-D-glucopyranoside (**2a**) and labeled a) methyl 1-[^{18}O]α-D-glucopyranoside (**12**) and b) methyl 1-[D]α-D-glucopyranoside (**13**). The negative peak of **12** appeared at 1141 cm^{-1}, lowered by 5 cm^{-1} compared to that of nonlabeled **2a** (at 1146 cm^{-1}). For **13**, a new small negative band appeared at 1136 cm^{-1}. The difference spectra were obtained by subtracting the isotopomer spectra from the spectrum of **2a**. VCD spectra were collected for 3 h.

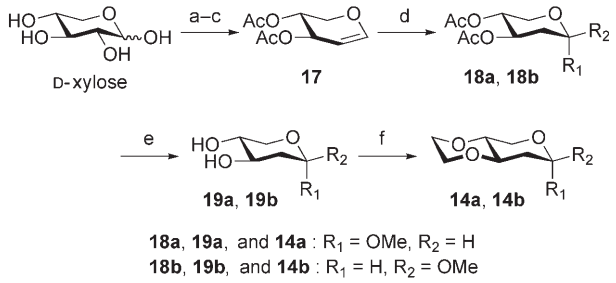

Scheme 2. Synthesis of the axial and equatorial model compounds. a) Ac$_2$O, pyridine, room temperature. b) HBr, AcOH, CH$_2$Cl$_2$, 0 °C. c) Zn, CuSO$_4$, CH$_2$Cl$_2$, H$_2$O, 0 °C. d) MeOH, TPHB, CH$_2$Cl$_2$, 0 °C, then separated. e) NaOMe, MeOH, room temperature. f) CH$_2$ClCH$_2$Cl, NaOH, H$_2$O, TBAB, 65 °C. These conditions were not optimized. TBAB = tetra-*n*-butylammonium bromide, TPHB = triphenylphosphine hydrobromide.

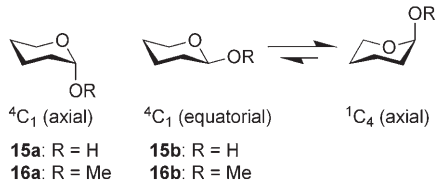

Scheme 3. Relationship between the simplest pyranose glycosidic models and their conformations: (*S*)-2-hydroxytetrahydropyran (**15a**), (*S*)-2-methoxytetrahydropyran (**16a**), and their enantiomers (**15b**, **16b**). The anomeric stereochemistry of **16** is fixed by the methyl substituent, whereas that of **15** is less stable because of the hemiacetal structure.

stretching vibration to approximately 2900 cm^{-1}.[20] Therefore, comparison of **2a** with both **12** and **13** supports a vibrational transition associated with more than two atomic oscillations that include H1, C1, and O1. To unravel this complicated vibrational motion, DFT calculations were performed next.

Design and Synthesis of the Axial and Equatorial Glycosidic Model Compounds

DFT predictions associated with experimental VCD spectroscopy reveal the absolute stereochemistry and conformation of various types of natural as well as synthetic molecules.[21] As mentioned before, however, simulation of carbohydrate VCD spectra was not successful except in a few cases,[22] due to the structural complexities and solvation factors involved. To simulate the vibrational mode of the glycoside band, we attempted to utilize a properly designed calculation-compatible model compound.

The resultant models **14a** and **14b** (Scheme 2) were designed to reflect the axial glycosidic feature that was expected to exhibit the glycoside band, as well as be simple, rigid, and soluble in a non-hydrogen-bonding solvent to enable reliable simulation. To simplify matters, most substituents were replaced by protons in the model, because the substituents have little influence on the glycoside band as discussed above. The simplest axial glycoside model would thus be (*S*)-2-methoxytetrahydropyran (**16a**; Scheme 3); however, its anomeric isomer **16b** cannot be an equatorial model, as **16b** is actually the enantiomer of **16a** and would not exist in the ^{4}C$_1$ conformation but would undergo a ring flip to take the ^{1}C$_4$ form (Scheme 3). We considered obtaining both axial and equatorial models that share a common backbone, to gain better insight by comparison of their VCD spectra. Therefore, the pyranose-ring conformations in **14a** and **14b** were fixed to the ^{4}C$_1$ conformation by a *trans*-decalin framework (Scheme 2). Two rings were fused at carbon atoms remote from C1 and connected through oxygen atoms to result in sugar-resembling structures.

The axial and equatorial model compounds **14a** and **14b** were prepared in an enantiomerically pure way starting from D-xylose. By following a standard procedure, D-xylal (**17**) was obtained in three steps (overall 34 %). Glycosidation of glycal with a catalytic amount of triphenylphosphine hydrobromide[23] was applied to **17** in the presence of 3 equivalents of methanol to give **18a** and **18b** in a 5:6 ratio (44 %).[24] Deacetylation of **18a** and **18b** yielded **19a** and **19b**, respectively. Their hydroxy groups 3-OH and 4-OH were bridged by using 1,2-dichloroethane to afford **14a** and **14b**, respectively, in moderate yields. The glycosidic structures of **14a** and **14b** were confirmed as axial and equatorial, respectively, by the coupling constants between the NMR signals of the anomeric and the vicinal protons (CDCl$_3$; **14a**: br d, $J_{H1,H2ax}$ = 3.5 Hz, H1; **14b**: dd, $J_{H1,H2ax}$ = 9.4 Hz, $J_{H1,H2eq}$ = 2.0 Hz, H1).[30] The synthetic intermediates **19a** and **19b** (methyl 2-deoxy-D-xylopyranosides), which were soluble in CDCl$_3$, were also studied to reinforce the discussion about the glycoside band.

Experimental and Theoretical VCD Spectra of 14a, 14b, and 19a: Vibrational Mode of the Glycoside Band

Conformational analysis of **14a** and **14b** by using MMFF94 and subsequent DFT optimization at the B3LYP/6-31G(d,p)

 © 2007 Wiley-VCH Verlag GmbH & Co. KGaA, Weinheim

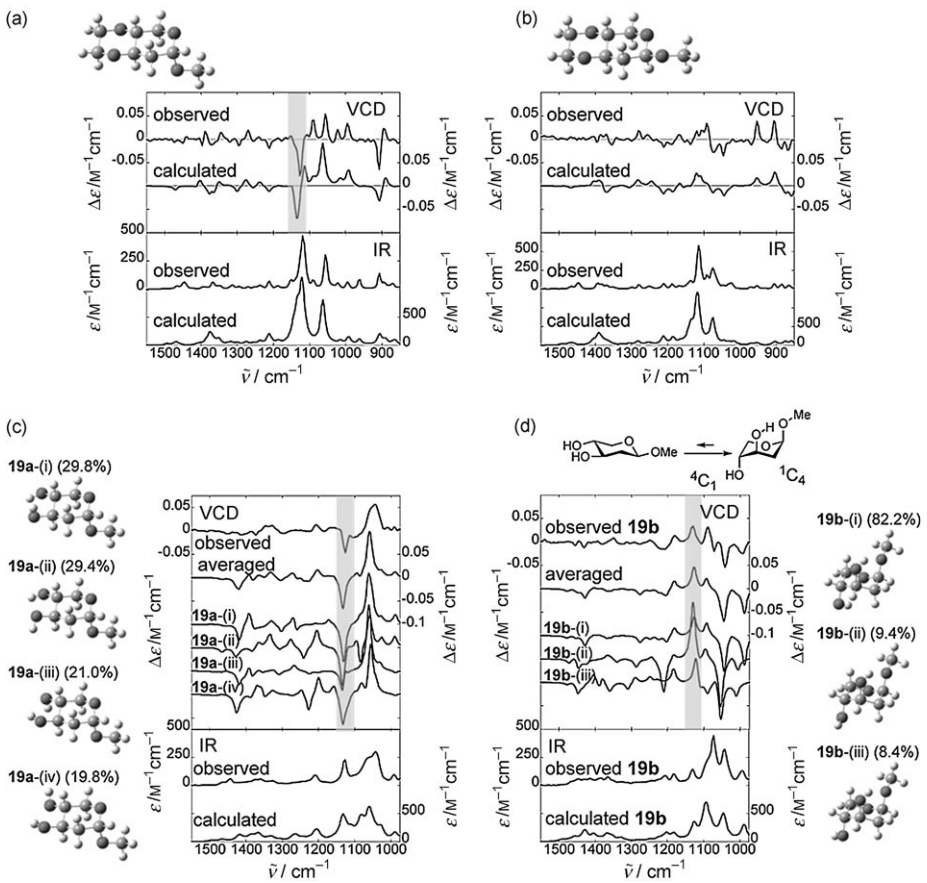

Figure 3. Calculated stable conformers and VCD (top) and IR spectra (bottom) of a) **14a** in CCl_4, 0.24 M, 46-μm BaF_2 cell, b) **14b** in CCl_4, 0.16 M, 46-μm BaF_2 cell, c) **19a** in $CDCl_3$, 0.10 M, 100-μm CaF_2 cell, and d) **19b** in $CDCl_3$, 0.10 M, 100-μm CaF_2 cell. For **19a** and **19b**, the theoretical spectra were obtained by averaging the spectra of each conformer according to the Boltzmann population shown in parentheses. The frequencies of the theoretical spectra were scaled by 0.98, the peak widths at half maximum were 8 cm^{-1} for a) and b) and 10 cm^{-1} for c) and d). The glycoside-band regions are highlighted in gray. VCD spectra were collected for 2 h.

level of theory led to only one stable conformer each. As expected, they exist in the $^4C_1$ pyranose-ring conformation, so the glycosidic methyl groups are directed axially and equatorially, respectively (Figure 3a and b). For the optimized conformer, VCD and IR spectra were simulated and compared with the experimental spectra obtained in CCl_4, which allowed observation up to 850 cm^{-1}. The axial glycoside model **14a** exhibited a sharp, negative, and strong peak in both the experimental and theoretical VCD spectra (Figure 3a). On the other hand, a weak, relatively flat peak was observed for the equatorial model **14b** (Figure 3b), thus indicating that the glycoside-band character is specific for axial glycosides. In other words, the anomeric configuration is also distinguishable in these model compounds by this band. The close agreement of the simulated spectra with the experimental shows, for the first time, that carbohydrate vibrational properties are predictable in a well-designed system.

To further our understanding about the vibrational nature of this band, axial α-glycosidic **19a** was also studied. After DFT optimization, four stable conformers were obtained. All of them take the $^4C_1$ conformation with an axial glycosidic linkage but differ in the orientation of their hydroxy groups. The VCD spectrum of each conformer was obtained by DFT calculation, and all showed the glycoside band. They were superimposed based on their Boltzmann population and compared with the spectrum obtained in $CDCl_3$; the two showed reasonable agreement (Figure 3c). Although the experimental VCD and IR spectra exhibited a broad and weak feature above 1100 cm^{-1} as observed in common carbohydrates, the glycoside band was well-maintained.

Scheme 4a and b shows the glycoside-band vibrational transitions of **14a** and the most stable conformer of **19a**, respectively. The arrows represent the degrees and orientations of each nuclear movement. For both **14a** and **19a**, the largest motion occurs at H1 and tends toward C1–H1 deformation rather than C1–H1 stretch. Whereas the movement of C1 is almost parallel to that of H1 in the same direction, O1 moves in the opposite direction, thus causing C–O stretch.[25] These vibrational features are consistent with the isotope experiments. On the other hand, as indicated by the systematic carbohydrate measurements, any contribution from the backbone other than C1 seems to be small or negligible. Consequently, the vibrational mode of the glycoside band was assigned as C1–H1 deformation coupled with C1–O1 stretch. The predicted coupling phenomenon is reasonable as vibrations of (hemi)acetal C–H deformation are known to be perturbed by C–O stretches.[26]

The assignment was further supported by the simulation of the isotope shifts of **14a** and **19a** (see Experimental Section). When O1 was replaced with ^{18}O, the shifts in the glycoside bands of **14a** and **19a** were estimated to be as small as 15 and 12 cm^{-1}, respectively, to lower frequency (Table 1). The band intensities were almost constant, thus reproducing the observed trends in ^{18}O-labeled **12**. On the other hand, deuteration simulation of H1 resulted in a remarkable VCD spectral change between 1200 and 1050 cm^{-1}: the disappearance of the glycoside band. Analysis of each vibrational mode indicated decoupling of C1–D1 deformation from C1–O1 stretching. A new, weak negative

 © 2007 Wiley-VCH Verlag GmbH & Co. KGaA, Weinheim

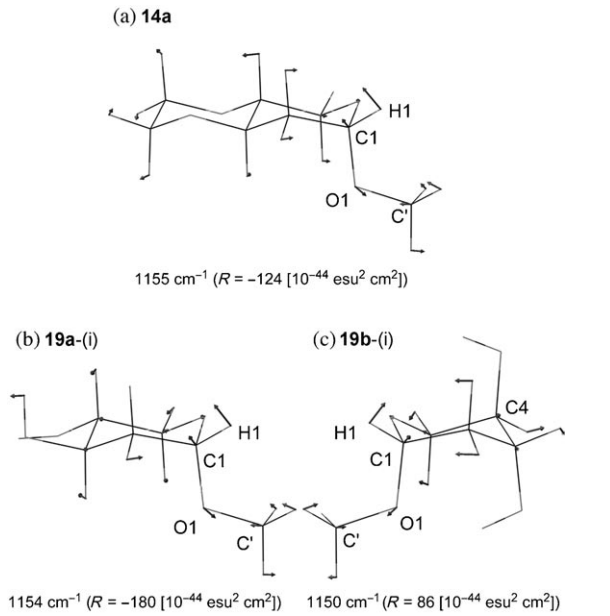

Scheme 4. Calculated vibrational mode at the glycoside band of a) **14a**, b) **19a**-(i), and c) **19b**-(i). The frequencies and rotational strengths R are shown below. The wavenumbers are not scaled. The arrows represent the degrees and directions of each nuclear movement.

Table 1. Observed and simulated isotope shifts.

Molecule (observed)	Frequency [cm^{-1}]	$\Delta\varepsilon$ [L mol^{-1} cm^{-1}]
2a	1146	−0.032
12 (1-[^{18}O]**2a**)	1141	−0.025
13 (1-[D]**2a**)	1136	−0.006

Molecule (simulated)	Frequency[a] [cm^{-1}]	R[b] [10^{-44} esu^{2}cm^2]	Dominant vibrations[c]
14a	1155	−124	δ C1–H1, ν_{as} C1–O1–C′
1-[^{18}O]**14a**	1140	−138	δ C1–H1, ν_{as} C1–O1–C′
1-[D]**14a**	1119	−71	δ C1–H1, ν C5–O5, δ –CH_2– (ethylene)
19a	1154	−180	δ C1–H1, ν_{as} C1–O1–C′
1-[^{18}O]**19a**	1142	−174	δ C1–H1, ν_{as} C1–O1–C′
1-[D]**19a**	1123	−26	δ C1–H1, ν C5–O5
14b	1190	21	δ C1–H1, ν_{as} C1–O1-C′, δ –CH_2– (C2), δ –CH_2– (C5)

[a] Predicted values without scaling. [b] Rotational strengths. [c] δ = deformation, ν = stretch, as = antisymmetric.

peak at around 1120 cm^{-1} was tentatively assigned as part of the glycoside-band vibrational mode recoupled with C5–O5 stretching. The simulated spectral feature agreed well with the experimental spectrum of deuterated **13**, in which the glycoside band was lost but a small negative band appeared at 1136 cm^{-1} instead.

To investigate the axial specificity of the glycoside band, vibrational modes of the equatorial **14b** were also analyzed. In calculated **14b**, vibrational motion corresponding to the glycoside band was not recognized near 1150 cm^{-1}, but vibration involving C1–H1 deformation and C1–O1–C′ stretching occurred at 1190 cm^{-1}, where it conjugated with methylene deformation to alter the vibrational character.[30] Hence, the axial specificity is primarily ascribed to a difference in frequency and consequent modification of the vibrational mode. In general, the stretching frequency is lowered in the presence of a factor that weakens the covalent bond.[26] For axial glycosidic sugars, the anomeric effect (donation from the axially oriented lone-pair electrons of O5 to the C1–O1 σ* orbital) decreases the C1–O1 bonding and lowers its stretching frequency relative to the equatorial species. Any factors that strengthen or weaken the C1–O1 linkage could shift the frequency of the glycoside band. If the shift is significantly large, C1–O1 stretch combines with other vibrations or decouples from C1–H1 deformation to result in a complete change of the VCD property in the glycoside-band region. Although the glycoside band is present for a variety of axial glycosides, we observed the disappearance of this band for those with carbonyl and aromatic substituents at the anomeric position (data not shown).

Positive Glycoside Band Exhibited by $^1C_4$ Sugars

Methyl 2-deoxy-β-D-xylopyranoside **19b** was also examined, and conformational analysis in the absence of solvent effects predicted that the three dominant conformers take the $^1C_4$ form with axial glycosidic linkages , despite **19b** being a β-D-sugar (Figure 3d). This is supported by the NMR coupling constants between the anomeric proton and the two vicinal protons in $CDCl_3$ ($J_{H1,H2ax}$ = 4.3 Hz, $J_{H1,H2eq}$ = 3.5 Hz). The solution of **19b** in $CDCl_3$ would therefore be an appropriate model for investigating the positive glycoside band observed in the $^1C_4$ conformation. The experimental VCD spectrum showed a broad and weak signal above 1150 cm^{-1} as with **19a** and the other sugars studied, whereas the positive glycoside band appeared just below 1150 cm^{-1} (Figure 3d). The overall VCD characteristic is in good agreement with that of the Boltzmann-weighted spectrum, including the glycoside band. The vibrational mode at the glycoside band was simulated as in Scheme 4c, in which the structure was reoriented to bring C1 to the front and take C4 to the back. In this mode, again, the C1–H1 deformation associated with the C1–O1–C′ asymmetric stretch was recognized, thus confirming that this type of vibration contributes to the glycoside band in both chair conformations. A comparison of the vibrational modes of **19a** and **19b** (Scheme 4b and c) showed that the nuclear motions around the anomeric center are almost mirror images of each other, in accordance with the opposite signs of the signals in their VCD spectra. In the calculated structure of **19b**, the anomeric oxygen atom was suggested to form a hydrogen bond with the hydroxy group at C3, but the glycoside band was observed irrespective of the presence of this bond, as shown in the VCD spectra of **19a** and **19b**.

Notably, the calculation-assisted VCD technique used herein clarified the preference of **19b** for the $^1C_4$ conformation over the $^4C_1$; this arrangement would place all hydroxy groups in less hindered equatorial positions. Here, the glyco-

 © 2007 Wiley-VCH Verlag GmbH & Co. KGaA, Weinheim

side band differentiated the conformation as well as the anomeric configuration. Although conformational analysis with VCD spectroscopy has been widely used in systems ranging from small molecules[21] to proteins and nucleic acids,[14] this is one of the first applications of this technique to the study of carbohydrate conformation.

Figure 4 summarizes the nature of the glycoside band as inferred from the results obtained so far. The glycoside band is defined as a sharp and intense VCD band near

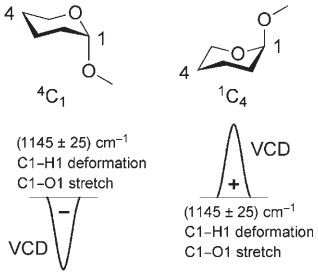

Figure 4. Summary of the glycoside band.

1145 cm^{-1}, exhibited by sugars with axial glycosidic linkages, with negative and positive signs for the $^4C_1$ and $^1C_4$ conformations, respectively, that arises from C1–H1 deformation coupled with C1–O1 stretching vibration.

Application to Glycoconjugates

Systematic observations and theoretical studies revealed that the vibrational movement of the glycoside band is almost independent of the substituent involved in the glycosidic linkage. This finding indicates that observation of the glycoside band in VCD spectra is applicable to studies of more-complicated glycoconjugates. In the first part of this paper, we mentioned that simple carbohydrates do not have carbonyl groups, in contrast to other biomolecules that have been studied with characteristic C=O-stretching VCD signals. The lack of carbonyl VCD signals in simple carbohydrates proves to be advantageous when glycoconjugates are analyzed. As the glycoside band is not based on carbonyl vibration, a simultaneous structural analysis of a carbohydrate and an aglycan moiety, such as peptide, protein, lipid, and others, can be conducted by focusing on both spectral regions.

Figure 5 shows the compatibility of the glycoside band with analysis of peptide secondary structure. Glycopeptide **20** is an antifreeze glycoprotein (AFGP) with a weight-average molecular weight of 6600 Da, which corresponds to 8–15 repeating units.[27] It was indicated that the antifreeze activity of AFGP is related to the polyproline type II (PPII)-like helical structure of the polypeptide backbone, and that this left-handed helix is regulated by the axial α-O-linked carbohydrate. To study these structural features, the VCD spectrum of **20** in water was obtained. As shown in Figure 5, **20** exhibited a negative glycoside band at 1165 cm^{-1} and an in-

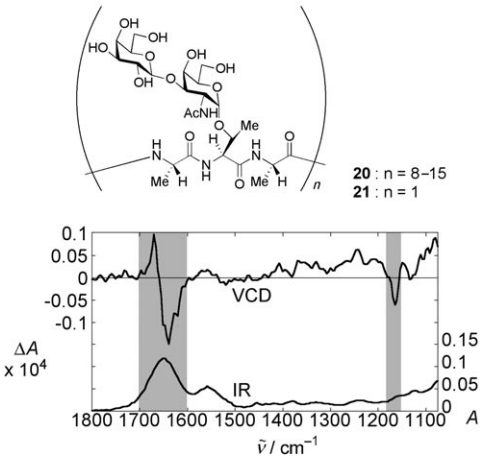

Figure 5. VCD and IR spectra of glycopeptide AFGP polymer **20** (500 mg mL^{-1} in H_2O, 6-μm CaF_2 cell, 2 h). The amide I VCD and glycoside bands are highlighted in gray.

tense negative–positive amide I VCD band characteristic of PPII-type secondary structure,[13a,28] thus confirming the PPII structural tendency previously suggested by electronic CD and NMR spectral studies.[27b] The PPII–amide VCD feature was also recognized in a solution of **20** in D_2O, whereas its tripeptide monorepeating unit **21** did not show any such characteristic feature.[30] This result with the polypeptide structure is consistent with the previous report, which predicted that a monomeric AFGP cannot take up an ordered conformation. Although two examples of glycoprotein VCD study have been reported so far,[29] this is the first VCD application to glycopeptides in which simultaneous structural elucidation of carbohydrates and polypeptides was also successfully carried out.

The broad applicability of the glycoside band was also demonstrated for other glycoconjugates such as glycolipids. Further VCD studies on glycoconjugates, including the simultaneous analysis of carbohydrate and aglycan parts, are in progress.

Conclusions

Through systematic carbohydrate VCD studies, we have characterized the glycoside band, the first unambiguous spectrum–structure correlation in carbohydrate VCD, as summarized in Figure 4. Isotope experiments and theoretical studies support the assignment of its vibrational mode as the C1–H1 deformation coupled with C1–O1 stretch. By starting from simple model compounds, reliable VCD predictions were first conducted on carbohydrates, including **19a** and **19b**, which contain flexible hydroxy groups. These results show that the complex vibrational nature of carbohydrates may be investigated by utilizing a properly designed system. These approaches may help in finding other structure-specific VCD features. We also used VCD spectroscopy for the first time in glycopeptide analysis and demonstrated the

 © 2007 Wiley-VCH Verlag GmbH & Co. KGaA, Weinheim

broad applicability of glycoside-band identification in VCD spectra to glycoconjugates. This study is expected to open new perspectives in glycoconjugate structure elucidation based on chiral information, which could play an important role in association with other methods such as NMR spectroscopy and MS, in the field of glycoscience.

Experimental Section

General Procedures

^{1}H (600 MHz) and ^{13}C NMR (150 MHz) spectra were recorded on a Bruker Avance spectrometer. Chemical shifts (δ) are reported in ppm relative to tetramethylsilane, and coupling constants (J) are in hertz. The following abbreviations are used for signal multiplicities: s = singlet, d = doublet, m = multiplet. EI MS was performed on a JEOL JMS-FABmate at the Center for Instrumental Analysis, Hokkaido University. Optical rotations were measured on a Perkin–Elmer 343 polarimeter with a 1-cm optical cell at ambient temperature. Analytical TLC was performed on 0.2-mm silica-gel plates (Merck 60 F-254), and column chromatography was carried out with silica gel (Kanto 60 N, 60–210 μm). HPLC purification was done on a Shimadzu LC-6A liquid chromatograph equipped with a Shimadzu RID-6A refractive-index detector and a CHIRALPAK® AD (1 cm $\phi \times 25$ cm) or CHIRALPAK® IA column (1 cm $\phi \times 25$ cm).

Preparation of Methyl Glycosides

^{18}O-labeled **12** was prepared from D-glucose and [^{18}O]methanol (purchased from Icon Isotopes) in the presence of a catalytic amount of acid as described in reference [14]. Methyl glycosides **2′a**, **2′b**, **5b**, **8a**, **8b**, **9a**, **10a**, and **10b** were prepared in a similar manner by using the corresponding sugars and methanol in the presence of DOWEX-50 H^+. The preparation of **13**, **14a**, **14b**, **19a**, and **19b** as well as their spectroscopic data are described in the Supporting Information. Compound **6a** was purchased from Toronto Research Chemicals as containing isopropanol and was used after having been evaporated twice from methanol. Other chemicals were purchased and used without further purification. AFGP polymer (**20**) and monomer (**21**) were kindly donated by Prof. Shin-Ichiro Nishimura and Dr. Yuki Tachibana of Hokkaido University.[27]

VCD Spectroscopy

VCD and IR spectra were obtained on a Bomem/BioTools Chiralir spectrometer with or without the second photoelastic modulator. All spectra were recorded at a resolution of 4 or 8 cm^{-1} at ambient temperature. Other conditions such as concentration, type of cell, solvent, and collection time are stated in the figure captions. Both VCD and IR spectra were corrected by a solvent spectrum obtained under the same experimental conditions.

Computation

The conformational distributions of **14a**, **14b**, **19a**, and **19b** were calculated by using MMFF94 systematic conformational searches with the Spartan 02 package,[31] followed by further optimization at the B3LYP/6–31G(d,p) level of theory without considering solvent effects, by using the Gaussian 03 package.[32] Conformer(s) within 2 kcal mol^{-1} from the most stable were taken into account for VCD/IR calculations at the same level of theory. VCD and IR spectra were simulated with Lorentzian lineshapes of 8- or 10-cm^{-1} width. Boltzmann populations were calculated by using ΔG values at 298 K. Final spectra were obtained based on the Boltzmann population average of each spectrum. Calculated nuclear displacements of the vibrational mode of interest were visualized with the GaussView program.

Isotope shifts were simulated by using the freqchk utility implemented in the Gaussian 03 package. Checkpoint files recorded in the calculations of **14a** and **19a**-(i) were used.

Acknowledgements

This work was supported in part by a Grant-in-Aid for scientific research (Grants 14658181, 16310144) from the Ministry of Education, Culture, Sports, Science, and Technology of Japan. We are grateful to Prof. Shin-Ichiro Nishimura and Dr. Yuki Tachibana for providing **20** and **21** and discussions, as well as Prof. Nobuaki Miura for discussions. T.T. gratefully acknowledges a scholarship from the Yoshida Scholarship Foundation (YKK Corp.) and a fellowship from the Japan Society for the Promotion of Science.

[1] a) A. Helenius, M. Aebi, *Science* **2001**, *291*, 2364–2369; b) P. M. Rudd, T. Elliott, P. Cresswell, I. A. Wilson, R. A. Dwek, *Science* **2001**, *291*, 2370–2376; c) H. Lis, N. Sharon, *Chem. Rev.* **1998**, *98*, 637–674; d) H.-J. Gabius, S. Andre, H. Kaltner, H-C. Siebert, *Biochim. Biophys. Acta* **2002**, *1572*, 165–177; e) M. E. Taylor, K. Drickamer, *Introduction to Glycobiology*, Oxford University Press, Oxford, **2003**.

[2] a) C.-H. Wong, *Carbohydrate-Based Drug Discovery*, Wiley-VCH, Weinheim, **2003**; b) B. O. Fraser-Reid, K. Tatsuta, J. Thiem, *Glycoscience*, Springer, Berlin, **2001**; c) J.-H. Kim, H. Yang, J. Park, G.-J. Boons, *J. Am. Chem. Soc.* **2005**, *127*, 12090–12097; d) D. Crich, N. S. Chandrasekera, *Angew. Chem.* **2004**, *116*, 5500–5503; *Angew. Chem. Int. Ed.* **2004**, *43*, 5386–5389.

[3] a) T. Kawano, J. Cui, Y. Koezuka, I. Toura, Y. Kaneko, K. Motoki, H. Ueno, R. Nakagawa, H. Sato, E. Kondo, H. Koseki, M. Taniguchi, *Science* **1997**, *278*, 1626–1629; b) B. Capon, *Chem. Rev.* **1969**, *69*, 407–498.

[4] J. Jiménez-Barbero, T. Peters, *NMR Spectroscopy of Glycoconjugates*, Wiley-VCH, Weinheim, **2003**.

[5] a) J. Zaia, *Mass Spectrom. Rev.* **2004**, *23*, 161–227; b) A. Dell, H. R. Morris, *Science* **2001**, *291*, 2351–2356; c) S.-I. Nishimura, K. Niikura, M. Kurogochi, T. Matsushita, M. Fumoto, H. Hinou, R. Kamitani, H. Nakagawa, K. Deguchi, N. Miura, K. Monde, H. Kondo, *Angew. Chem.* **2005**, *117*, 93–98; *Angew. Chem. Int. Ed.* **2005**, *44*, 91–96; d) N. C. Polfer, J. J. Valle, D. T. Moore, J. Oomens, J. R. Eyler, B. Bendiak, *Anal. Chem.* **2006**, *78*, 670–679.

[6] S. B. Levery, S.-I. Hakomori, *Methods Enzymol.* **1987**, *138*, 13–25.

[7] For a modified permethylation analysis combined with MS or electronic CD, see: a) I. Ciucano, *Anal. Chim. Acta* **2006**, *576*, 147–155; b) W. T. Wiesler, N. Berova, M. Ojika, H. V. Meyers, M. Chang, P. Zhou, L.-C. Lo, M. Niwa, R. Takeda, K. Nakanishi, *Helv. Chim. Acta* **1990**, *73*, 509–551.

[8] C. S. Hudson, *J. Am. Chem. Soc.* **1909**, *31*, 66–86.

[9] a) R. K. Dukor, L. A. Nafie in *Encyclopedia of Analytical Chemistry* (Ed.: R. A. Meyers), John Wiley & Sons, Chichester, **2000**, pp. 662–676; b) L. A. Nafie, T. B. Freedman in *Circular Dichroism: Principles and Applications*, *2nd ed.* (Eds.: N. Berova, K. Nakanishi, R. W. Woody), Wiley-VCH, New York, **2000**, pp. 97–131; c) P. L. Polavarapu, J. He, *Anal. Chem.* **2004**, *76*, 61A–67A.

[10] For a recent review on carbohydrate VCD studies, see: T. Taniguchi, K. Monde, *Trends Glycosci. Glycotech.* **2007**, *19*, 147–164.

[11] a) A. F. Bell, L. Hecht, L. D. Barron, *J. Am. Chem. Soc.* **1994**, *116*, 5155–5161; b) F. Zhu, N. W. Isaacs, L. Hecht, L. D. Barron, *J. Am. Chem. Soc.* **2005**, *127*, 6142–6143.

[12] a) D. M. Back, P. L. Polavarapu, *Carbohydr. Res.* **1984**, *133*, 163–167; b) C. M. Tummalapalli, D. M. Back, P. L. Polavarapu, *J. Chem. Soc. Faraday Trans. 1* **1988**, *84*, 2585–2594; c) P. K. Bose, P. L. Polavarapu, *Carbohydr. Res.* **1999**, *319*, 172–183; d) P. K. Bose, P. L. Polavarapu, *J. Am. Chem. Soc.* **1999**, *121*, 6094–6095.

[13] a) T. A. Keiderling in *Circular Dichroism: Principles and Applications*, *2nd ed.* (Eds.: N. Berova, K. Nakanishi, R. W. Woody), Wiley-VCH, New York, **2000**, pp. 621–666; b) T. A. Martinek, I. M. Mándity, L. Fülöp, G. K. Tóth, E. Vass, M. Hollósi, E. Forró, F. Fülöp, *J. Am. Chem. Soc.* **2006**, *128*, 13539–13544; c) A. Annamalai, T. A. Keiderling, *J. Am. Chem. Soc.* **1987**, *109*, 3125–3132; d) A. Polyanichko, H. Wieser, *Biopolymers* **2005**, *78*, 329–339; e) V. Set-

 © 2007 Wiley-VCH Verlag GmbH & Co. KGaA, Weinheim

nicka, M. Urbanová, K. Volka, S. Nampally, J.-M. Lehn, *Chem. Eur. J.* **2006**, *12*, 8735–8743.
[14] a) P. Bour, T. A. Keiderling, *J. Am. Chem. Soc.* **1993**, *115*, 9602–9607; b) R. Huang, J. Kubelka, W. Barber-Armstrong, R. A. G. D. Silva, S. M. Decatur, T. A. Keiderling, *J. Am. Chem. Soc.* **2004**, *126*, 2346–2354; c) J. Kubelka, R. Huang, T. A. Keiderling, *J. Phys. Chem. B* **2005**, *109*, 8231–8243; d) K.-K. Lee, S. Hahn, K.-I. Oh, J. S. Choi, C. Joo, H. Lee, H. Han, M. Cho, *J. Phys. Chem. B* **2006**, *110*, 18834–18843; e) A. T. Krummel, M. T. Zanni, *J. Phys. Chem. B* **2006**, *110*, 24720–24727.
[15] K. Monde, T. Taniguchi, N. Miura, S.-I. Nishimura, *J. Am. Chem. Soc.* **2004**, *126*, 9496–9497.
[16] J. R. Cheeseman, M. J. Frisch, F. J. Devlin, P. J. Stephens, *Chem. Phys. Lett.* **1996**, *252*, 211–220.
[17] It has to be emphasized that another recently reported characteristic VCD peak in the C–H stretching region was governed by the *R*/*S* representation instead of the D/L, α/β, $^4C_1/^1C_4$, or axial/equatorial. In the current study, we systematically examined the glycoside band to avoid misinterpretation. For *R*/*S*-dependent VCD, see: T. Taniguchi, K. Monde, N. Miura, S.-I. Nishimura, *Tetrahedron Lett.* **2004**, *45*, 8451–8453.
[18] a) V. Setnicka, R. Huang, C. L. Thomas, M. A. Etienne, J. Kubelka, R. P. Hammer, T. A. Keiderling, *J. Am. Chem. Soc.* **2005**, *127*, 4992–4993; b) A. A. Pandyra, A. P. Yamniuk, V. V. Andrushchenko, H. Wiesler, H. J. Vogel, *Biopolymers* **2005**, *79*, 231–237.
[19] H. Günzler, H.-U. Gremlich, *IR Spectroscopy*, Wiley-VCH, Weinheim, **2002**, pp. 14–17.
[20] T. Taniguchi, K. Monde, *Org. Biomol. Chem.* **2007**, *5*, 1104–1110.
[21] a) T. B. Freedman, X. Cao, R. K. Dukor, L. A. Nafie, *Chirality* **2003**, *15*, 743–758; b) M. Urbanová, V. Setnicka, F. J. Devlin, P. J. Stephens, *J. Am. Chem. Soc.* **2005**, *127*, 6700–6711; c) T. Furo, T. Mori, T. Wada, Y. Inoue, *J. Am. Chem. Soc.* **2005**, *127*, 8242–8243; d) T. Brotin, D. Cavagnat, J.-P. Dutasta, T. Buffeteau, *J. Am. Chem. Soc.* **2006**, *128*, 5533–5540; e) K. Monde, N. Miura, M. Hashimoto, T. Taniguchi, T. Inabe, *J. Am. Chem. Soc.* **2006**, *128*, 6000–6001; f) H. Izumi, S. Futamura, N. Tokita, Y. Hamada, *J. Org. Chem.* **2007**, *72*, 277–279.
[22] a) M. W. Ellzy, J. O. Jensen, H. F. Hameka, J. G. Kay, *Spectrochim. Acta A* **2003**, *59*, 2619–2633; b) N. Miura, T. Taniguchi, K. Monde, S.-I. Nishimura, *Chem. Phys. Lett.* **2006**, *419*, 326–332.
[23] V. Bolitt, C. Mioskowski, *J. Org. Chem.* **1990**, *55*, 5812–5813.
[24] Their NMR spectra were almost identical with reported data: a) W. H. Binder, R. H. Prenner, W. Schmid, *Tetrahedron* **1994**, *50*, 749–758; b) P. Biely, M. Mastihubová, *Carbohydr. Res.* **2004**, *339*, 2101–2110.
[25] In these models, the stretching mode was more like the C1–O1–C′ antisymmetric vibration, although the glycoside band also appeared in hemiacetal structures such as **2c**, **3**, and **11a**. We further calculated the vibrational mode of free axial glycosidic **15a** (Scheme 3), and the result suggests that C′ is not necessary to exhibit the glycoside band (data not shown).
[26] G. Socrates, *Infrared and Raman Characteristic Group Frequencies, 3rd ed.*, John Wiley & Sons, Chichester, **2001**, pp. 101–104.
[27] a) Y. Tachibana, N. Matsubara, F. Nakajima, T. Tsuda, S. Tsuda, K. Monde, S.-I. Nishimura, *Tetrahedron* **2002**, *58*, 10213–10224; b) Y. Tachibana, G. L. Fletcher, N. Fujitani, S. Tsuda, K. Monde, S.-I. Nishimura, *Angew. Chem.* **2004**, *116*, 874–880; *Angew. Chem. Int. Ed.* **2004**, *43*, 856–862.
[28] R. K. Dukor, T. A. Keiderling, *Biopolymers* **1991**, *31*, 1747–1761.
[29] a) G. Shanmugan, P. L. Polavarapu, *Proteins: Structure, Function, and Bioinformatics* **2006**, *63*, 768–776; b) M. Urbanova, P. Pancoska, T. A. Keiderling, *Biochim. Biophys. Acta* **1993**, *1203*, 290–294.
[30] See Supporting Information for more details.
[31] Spartan 02, to be found under http://www.wavefun.com, **2002**.
[32] M. J. Frisch, G. W. Trucks, H. B. Schlegel, G. E. Scuseria, M. A. Robb, J. R. Cheeseman, J. A. Montgomery, T. Vreven, K. N. Kudin, J. C. Burant, J. M. Millam, S. S. Iyengar, J. Tomasi, V. Barone, B. Mennucci, M. Cossi, G. Scalmani, N. Rega, G. A. Petersson, H. Nakatsuji, M. Hada, M. Ehara, K. Toyota, R. Fukuda, J. Hasegawa, M. Ishida, T. Nakajima, Y. Honda, O. Kitao, H. Nakai, M. Klene, X. Li, J. E. Knox, H. P. Hratchian, J. B. Cross, C. Adamo, J. Jaramillo, R. Gomperts, R. E. Stratmann, O. Yazyev, A. J. Austin, R. Cammi, C. Pomelli, J. W. Ochterski, P. Y. Ayala, K. Morokuma, G. A. Voth, P. Salvador, J. J. Dannenberg, V. G. Zakrzewski, S. Dapprich, A. D. Daniels, M. C. Strain, O. Farkas, D. K. Malick, A. D. Rabuck, K. Raghavachari, J. B. Foresman, J. V. Ortiz, Q. Cui, A. G. Baboul, S. Clifford, J. Cioslowski, B. B. Stefanov, G. Liu, A. Liashenko, P. Piskorz, I. Komaromi, R. L. Martin, D. J. Fox, T. Keith, M. A. Al-Laham, C. Y. Peng, A. Nanayakkara, M. Challacombe, P. M. W. Gill, B. Johnson, W. Chen, M. W. Wong, C. Gonzalez, J. A. Pople, Gaussian 03 (Revision C.02), Gaussian, Inc., Wallingford, CT (USA), **2004**.

Received: May 28, 2007
Published online: September 4, 2007

 © 2007 Wiley-VCH Verlag GmbH & Co. KGaA, Weinheim